CORROSION-INDUCED BOND BEHAVIOUR OF STEEL, E-GLASS, AND E-WASTE COPPER WIRE FIBER REINFORCED CONCRETE

GANESH NAIDU GOPU, A. SOFI*

, Department of Structural and Geotechnical Engineering, School of Civil Engineering, Vellore Institute of Technology, Vellore 632014, India

The chloride attack on the reinforced concrete structure resulted in a substantial loss of bond strength due to reinforcing bar corrosion. E-glass, Steel and E-waste copper fibers were used in concrete to investigate corrosion-induced bonding behaviour. It was determined to perform pull-out tests in order to evaluate the bond behavior in relation to test variables such as the ratio of concrete cube clear cover (C) to rebar diameter (Ø) and the type of fiber. The bond stress-slip curves produced in this work adequately represented the bond behavior of corroded and uncorroded concrete specimens (with and without fibers). According to the findings, adding fibers to concrete appears to strengthen the connection and reduce corrosion. The bond strength of steel fiber reinforced concrete was found to be higher than that of concrete mixes including E-glass and E-copper wire fibers.

Keywords: *Chloride attack; Bond strength; Corrosion-induced; pull out test; corrosion rate; chloride attack*

1. Introduction

Chloride attack results in rebar corrosion in many marine-exposed reinforced concrete structures. The steel rebar had corroded and was bulging outward [1]. Numerous studies have discovered that the tensile strength of reinforcing bars is lowered as a consequence of the reduction in the cross-sectional area of the rebar, which occurs as a result of corrosion. A substantial influence on the bonding efficiency between the steel rebar and the concrete matrix was caused by the corrosion of the steel rebar and the surrounding concrete matrix [2]. The addition of fibers to concrete can significantly increase the bonding behaviour between rebar and concrete. Introducing fiber containment into concrete reduced bond breakdown while also increasing energy dissipation under cyclic load processing. The current experiment comprised the introduction of three types of fibers into the concrete mix, including E-glass, steel, and E-waste copper wire fibers, in order to evaluate the bonding behaviour of the concrete when exposed to chloride ions. The corrosion-resistant properties of copper wire fibers derived from e-waste are being used as a novel concrete additive. Copper wire fibers obtained from electrical and electronic trash, such as electrical wires, telephone cables, computers, fans, and mortars, among other things, are used to create e-waste. E-waste is a term that refers to garbage generated by the recycling of copper wire fibers[3][4]. Originally, E-glass fiber was considered an electronic waste that would influence the environment because it is non-biodegradable[5]. Concrete fibers made from electrical waste are stronger and more durable than regular concrete. Concrete with E-glass fibers has better bond strength and electrical resistance.[6].Steel rebar incorporated in SFRC has proven to be more durable than ordinary concrete in chloride-exposed experiments, according to the findings of those investigations. Furthermore, an accelerated corrosion process was adopted in this study, which differs from normal corrosion[7]. First and foremost, unique corrosion and swelling effects were found during accelerated corrosion due to inadequate oxidation. In addition, faster corrosion results in more consistent rebar corrosion. Third, during accelerated corrosion, the dissipation of corrosion products to the surrounding SFRC and leaching into corrosion-induced fractures requires less time. Using the pullout test, you can see how well steel rebar connects to the concrete matrix and how strong the concrete is to it.[8].

The purpose of this paper was to determine the electrical resistivity of various concrete mixes, the corrosion-induced bond behaviour of steel rebar and the surrounding concrete matrix (with and without fibers), and to determine the corrosion level of reinforced concrete matrix reinforced with steel, E-glass, and E-waste copper fibers.

2.Exerimental procedure

2.1. *Materials used and concrete mix*

Ordinary Portland cement of grade 53 was used. Granite crushed to 20 mm was used as the coarse aggregate and its density was 1540 kg/m^3, and its fineness modulus was 4.32, river sand of its fineness modulus 2.8 was used and its bulk density was 1780 kg/m^3. Steel fibers of length 40 mm and diameter 0.8 mm were used, E-waste copper wire fiber (CF) of 30mm length and 0.6mm diameter and E-glass fiber (GF) of 6mm length and 0.12mm diameter were used for this study. The concrete mix proportion was developed in accordance with the BIS code[9]. A w/c ratio of 0.45 was used with a concrete mix proportion of M40 grade of 1:1.71:2.39 Three distinct fibers, such as SF,CF and GF are randomly injected into the concrete at a volume

*Autor corespondent/*Correspondingauthor*,
E-mail:asofi@vit.ac.in

Table 1

Rebar surface geometries

Diameter of the rebar (mm)	Transverse Rib				Longitudinal Rib		Bond minimum rib area, $f_{R\,min}$ (EN 1992-1-1 code)
	Average Rib Height (mm)	Rib inclination	Rib spacing(mm)	Rib area(mm^2)	Average height(mm)	Average Rib base width (mm)	
12	0.55	51.5	7.5	0.037	0.90	3.0	0.040
16	0.95	67.0	9.3	0.051	1.40	2.05	0.056

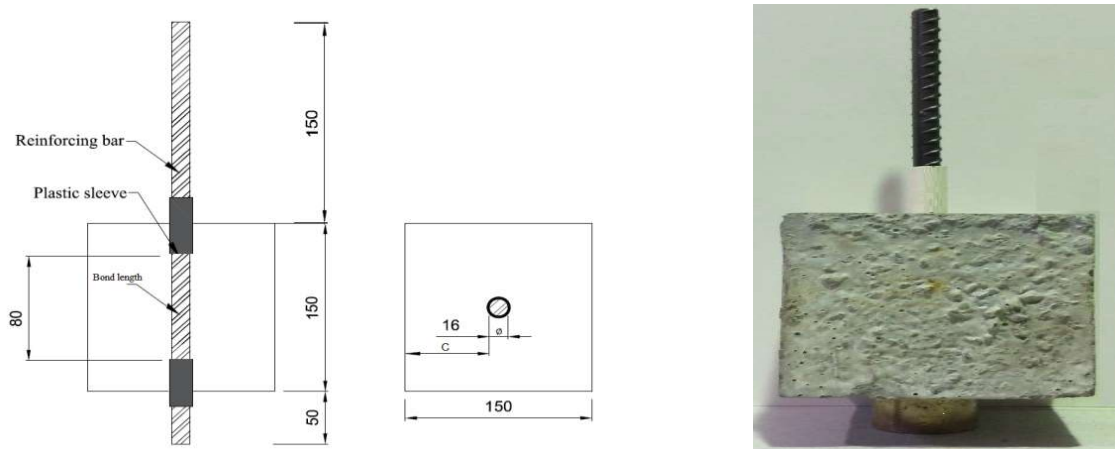

Fig.1.- Setup for pull-out specimens: (a) Specifications for pull-out specimens, (b) Pull-out specimen

Table 2

Concrete mix types

Stages of corrosion	Specifies the kind of concrete mix to use				
	CF	GF	SF	N	Series
Corroded	Ø12-CF-5.75-Cor	Ø12-GF-5.75-Cor	Ø12-SF-5.75-Cor	Ø12-N-5.75-Cor	C/Ø =5.75
	Ø16-CF-4.19-Cor	Ø16-GF-4.19-Cor	Ø16-SF-4.19-Cor	Ø16-N-4.19-Cor	C/Ø =4.19
Non-corroded	Ø12-CF-5.75-Ref	Ø12-GF-5.75-Ref	Ø12-SF-5.75-Ref	Ø12-N-5.75-Ref	C/Ø =5.75
	Ø16-CF-4.19-Ref	Ø16-GF-4.19-Ref	Ø16-SF-4.19-Ref	Ø16-N-4.19-Ref	C/Ø =4.19

fraction of 1% each. The fibers always been integrated and mixed for the shortest period of time possible in order to ensure uniform dispersion and minimize damage from over mixing.

2.2.Sample preparation and testing

For the purpose of examining the binding behavior of steel bars to the underlying concrete mix with and without fiber, 48 specimens were tested. There were two different stages of corrosion employed to study the bonding behavior: the uncorroded stage and the corroded stage. The pull-out experiment was used to estimate the bond strength. IS 2770(part1) was used to prepare and evaluate the samples [10]. It was determined that the specimens had a 150 mm cube shape and were reinforced with high yield strength deformed steel rebars of 12 and 16 mm diameters, with the surface geometries of the steel rebars given in Table 1.The rebar was placed along their centre lines shown in Fig.1.According to the plans, the concrete cube transparent cover thickness (C) to steel rebar diameter (Ø) ratios would be 5.75 and 4.19 respectively. The central piece (in between the top and bottom plastic slives) was designated as a bond length, while the two ends were designated as non-bonding sections (as seen in the diagram). As seen in Fig. 1, a PVC tube is utilized to protect the reinforcing segment of the non-bonding zone. We adopted a rebar bond length that was five times the diameter of the rebar (60 mm and 80 mm). In order to cast concrete cube specimens, we used plywood molds. The specimens were covered with plastic sheets to prevent moisture loss, and specimen data with coding was displayed in Table 2.

2.3.Setup for experimentation

A total of two stages of tests were carried out in the current research. Before any corrosion cracking could occur, the specimens were exposed to accelerated corrosion to determine the start and propagation of corrosion cracks. Second, over the course of the testing, the specimens' bond strength and corrosion level were both measured.

2.3.1.Test for accelerated corrosion

Impressed direct current (DC) was employed for corrosive reinforcement in accelerated corrosion testing since it is an easier

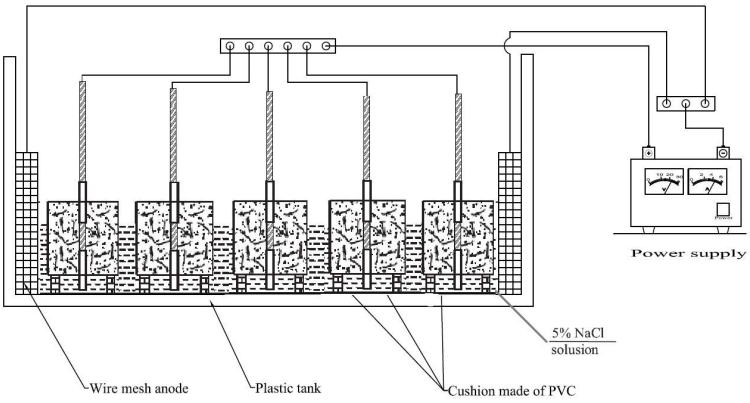

Fig.2 - Accelerationcorrosion test setup

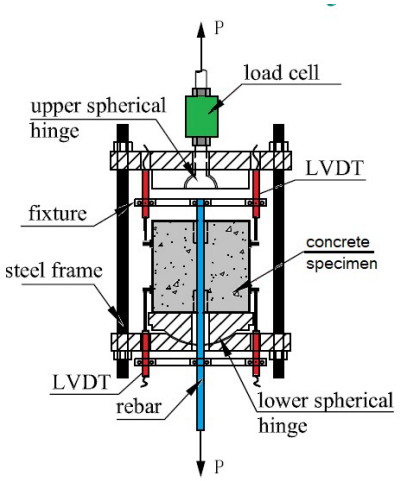

Fig.3-Pull out test

way. Corrosion on naturally corroded structures can produce crack splitting, which can take a long time to observe. The samples were immersed for three days in a plastic tank filled with NaCl solution to ensure that they received the highest amount of saturation possible before being exposed to fast degradation. To accelerate the corrosion process, a 30-volt continuous potential and an 0-4 amp direct current source were employed in conjunction with each other[11]. Using the steel bars as anodes, which were embedded in the concrete, direct current was applied. The cathode was made up of galvanized mesh that was submerged in the NaCl solution across the specimens in order to cause the variations from the implanted steel rebar to the galvanized mesh submerged in the NaCl solution depicted in the Fig.2 The maximum current density for rebar in highly cracked concrete was 100 μA/cm^2 when the concrete was significantly cracked. During all of the accelerated corrosion experiments, the electrical resistance of each specimen was measured on an hourly basis with the use of a multimeter in order to detect when cracking was induced by corrosion on the specimen. Through the use of an ammeter and a data recorder, the current fluctuation between the cathode and the anode was monitored and recorded once an hour. The crack parameters were measured with the help of a crack gauge. After removing the concrete specimens from the plastic tank, they were put in a container filled with drinking water until the pull-out test was conducted.

2.3.2. Pull-out test

Pull-out tests were performed using 300 kN electro-hydraulic testing equipment. The pull-out load was applied in various loading modes and speeds. The loading frame and the test setup were shown in Fig.3. Sphere hinges were installed on the top and bottom endplates of the loading frame in order to give central tensile strength. Measurement of the pull-out load between the loading frame and the testing machine was carried out using a 100 kN load cell. It was necessary to use two sets of linear variable difference transformers in order to record the circumstances at the rebar concrete slippage interface. a static data-gathering system that is computer-based[12]. The bonding strength (τ) of the specimens was determined by applying Eq (1).

$$\tau = \frac{P}{\pi \emptyset L} (1)$$

When P is the applied pull in Newton's, Ø is the steel rebar diameter in millimetres (mm), and L is the bond length of the reinforcing steel bar in millimetres (mm), the bond strength is given in MPa

Bond: Where it can be shown that sufficient bond strength is achievable with f_R values less than specified above, the values may be relaxed. In order to ensure that sufficient bond strength is achieved, the bond stresses should satisfy the recommended equation (2) as per EN 1992-1-1 code

$$\tau \geq 0.098(130 - 1.9\,\emptyset) \quad (2)$$

2.3.3. Reinforcement corrosion severity (corrosion rate)

After the pull-out test, the steel rebar was ejected from the concrete specimen and cleaned to assess gravimetric steel loss. In accordance with ASTM G1-03, the rebar bond portion was cut and plunged into a 12 percent HCl solution to remove rust products.[13]. Eq. (3) yields the actual corrosion level (*υ) in %*.

$$\upsilon = \frac{\Delta m * L_t}{m_0 * L_b} * 100 \quad (3)$$

Where Δm is the corrosion induced mass loss, m_0 is the weight of the steel rebar before it was cast, $L_b$is the bonded length of the rebar and L_t is the total rebar length.

3.Results and discussion

3.1.Behaviour of corrosive cracking

During corrosion, the positively charged steel bars attract negative chloride ions from the

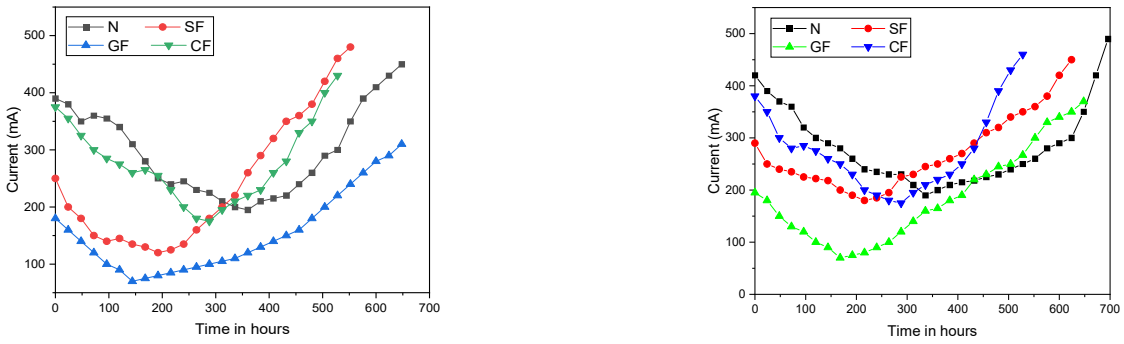

Fig.4 -Time tocorrosionandcrackingindicationcurves (a) C/Ø of 5.75, (b) C/Ø of 4.19

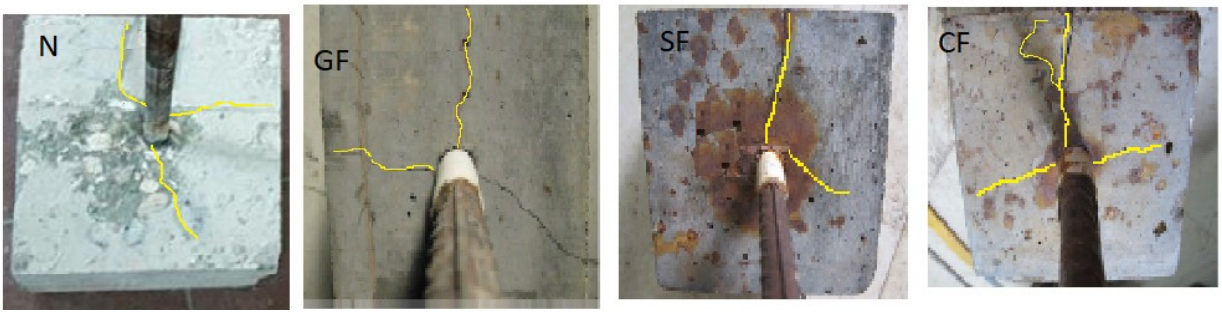

Fig. 5 – Corrosion crack pattern

NaCl solution. When the chloride ions got to the steel rebar, the surface started to corrode. Brown rust was seen on the specimens' upper surfaces, indicating that corrosion had begun on the embedded rebar. This is known as the initiation stage of corrosion. It was discovered that ordinary concrete cracks were present in this instance, whereas reinforced concrete does not show any cracks. The current passing through concrete specimens was reduced for 140-400 hours after the current starts to rise and for the next 72-96 hours as demonstrated in Fig.4.The initial current decrease was most likely caused by NaCl solution deposits filling up the concrete's pore spaces[14]. Corrosion may have started on embedded rebar, based on the increase in current flow. There were lower initial current values for fiber-reinforced concrete specimens compared to standard-concrete ones. E-glass fiber inclusion in concrete mixtures had a lower reading than in the other mixtures. Compared to other concrete combinations, E-glass reinforced concrete has increased resistance to chloride penetration. Cracking began when the current supply was increased from 1.8 to 4.0 Amps. Finally, as indicated in Fig.5 the specimens' crowns exhibited a crack pattern. There were numerous fissures in each of the buildings, with one being much larger than the others. The principal crack in (Fig.5) is depicted in this figure with a thicker line width, and the crack width of each specimen is determined on the top surface[15].

3.2.Mode of bond failure

It was discovered that three types of failure modes occurred during the pull-out test: splitting mode, pull-out mode, as well as a combination of splitting and pull-out mode.[16]. Concrete matrix tension characteristics surrounding the rebar determined the primary mode of failure. When tested under maximum stress, every typical concrete mix specimen is split into two parts[10]. Additionally, specimens of C/Ø of 5.25 series, as well as SF and CF integrated concrete, failed when pulled out. When the rebar was pulled out, it developed longitudinal and radial cracks. Pull-out and splitting failure modes coexisted in the GF inclusion concrete mix specimens that failed. Concrete scattered E-glass fibers are mostly to blame for this increase in strength and ductility. It was decided to employ all of the specimens in the combined effect of the pull-out and splitting failure modes used for C/Ø of the 4.19-series. As the test samples reached their maximum load, the splitting crack appeared on the load-carrying side and subsequently grew and formed to the free end with increasing slide. Fiber-reinforced concrete's enhanced tension and ductility are substantially to blame. The specimens' bond failure patterns are displayed in Fig.6.The comparison with Fazli et al. [17] result on C/Ø of 5.25 series specimens can increase the confinement effect.

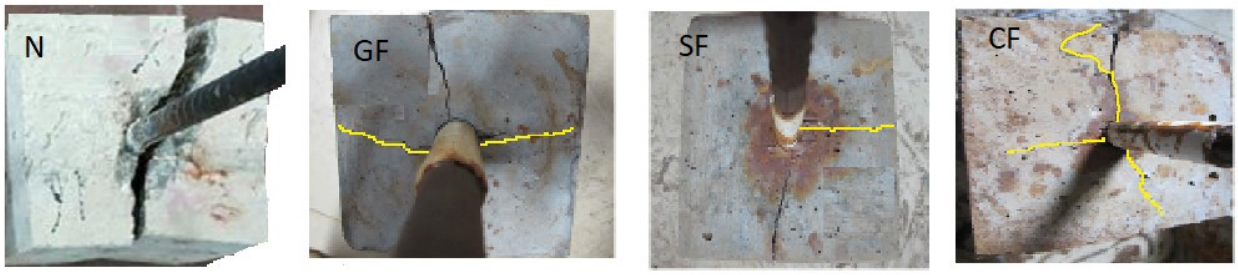

Fig. 6 – Bond failure mode

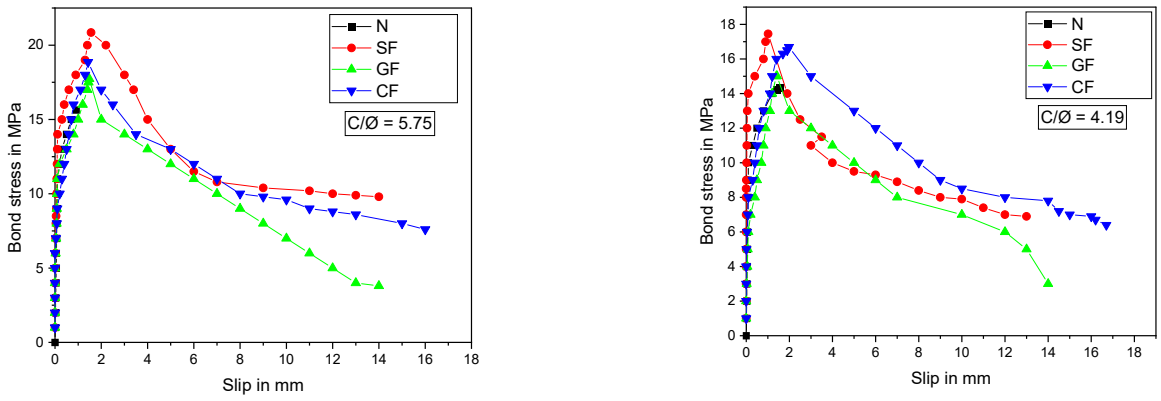

a b

Fig. 7 - Uncorroded specimen bond stress slip curves : (a) C/Ø of 5.75, (b) C/Ø of 4.19

3.3.Bond-slip curves

Each stage of the bond-slip curve is represented by a curve segment: rising, falling, and residual. The bond-slip curve was impacted by two variables: concrete specimen (C/Ø) ratio and concrete fiber type. They have a significant impact on bond performance during periods of peak load. Fig.7 depicts uncorroded concrete bond stress-slip curves; it is immediately apparent that traditional concrete specimens have a raising stage, While specimens of fiber reinforced concrete go through three distinct phases: increasing, falling, and residual (see Fig.7). Using the series of C/Ø = 5.75, the E-waste copper wire fiber inclusion concrete mix specimens revealed trustworthy non-linear slip behaviour around the ultimate bonding stress when compared to the concrete mixes that had been employed in the previous investigations, the results showed in Fig.9 With the exception of C/Ø = 4.19, a significant decrease in bond stress was detected at the apex level, and this decrease was shown to be rising with decreasing C/Ø ratio. The mechanism of failure was the most significant factor in this decrease. After being implanted in steel and E-waste copper wire fibers with a C/Ø = 5.75 ratio, even so, the inserted steel rebar was kept tightly contained by the surrounding steel fibers, and it showed no signs of splitting. The maximal bond tension in a given slip may be maintained for a limited period of time until the degradation of the fiber between the rebar ribs renders the steel rebar's interlocking action with the reinforced fiber concrete ineffective. a Combined splitting and pull-out failure were the modes of failure for E-glass fiber incorporated concrete specimens with C/Ø = 5.75 and C/Ø = 4.19 series of all concrete mix specimens with C/Ø = 4.19. Due to a splitting crack at the peak load, the surrounding matrix containment has been weakened, leading in a combination of splitting and pull-out failure. The resistance of the rebar to the surrounding matrix was the primary reason for the residual bond strength. The residual bond strength of uncorroded concrete specimens was enhanced by increasing the C/Ø ratio. The bond-slip curves for deteriorated concrete were depicted in this Fig.8. Significantly influenced the stress-slip behaviour of the bond was corrosion caused by steel reinforcement bars. The bond stresses and peak bond stresses of the corroded concrete specimens were smaller than those of the uncorroded specimens at the peak point, and the rise in C/Ø lengthened the duration of bond losses. The decreasing gradient of the bond stress reduced as the corrosion rate, notably for the C/Ø = 5.75. When C/Ø = 4.19 is used, a reduction in bond stress at the peak point is seen in all specimens. The mechanical interlocking mechanism was largely responsible for the loss of bond strength, which was caused by the corrosion of the rebar ribs. As corrosion progressed for smaller-diameter rebar, rib damage became more severe. In the instance of the series C/Ø= 5.75, a greater loss of bond stiffness was seen compared

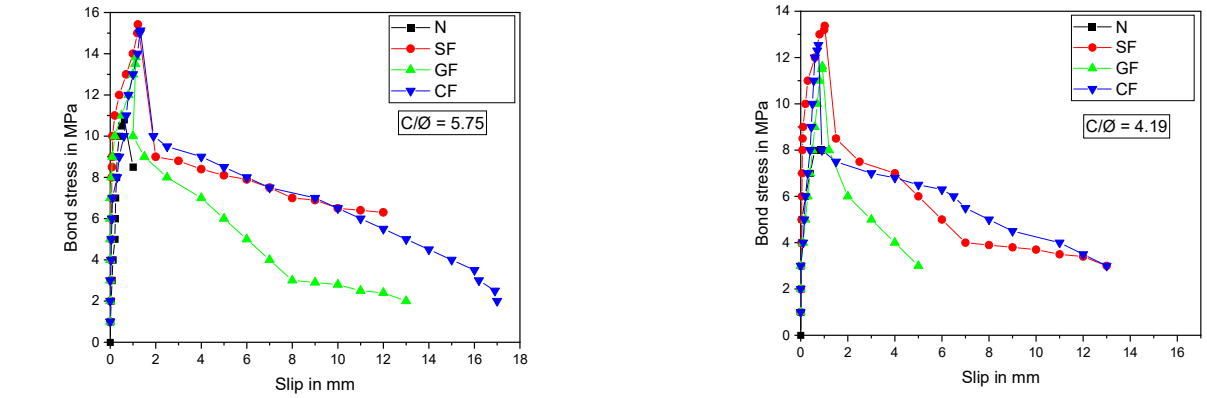

A b

Fig. 8 - Corroded specimen bond stress slip curves: (a) C/Ø of 5.75, (b) C/Ø of 4.19

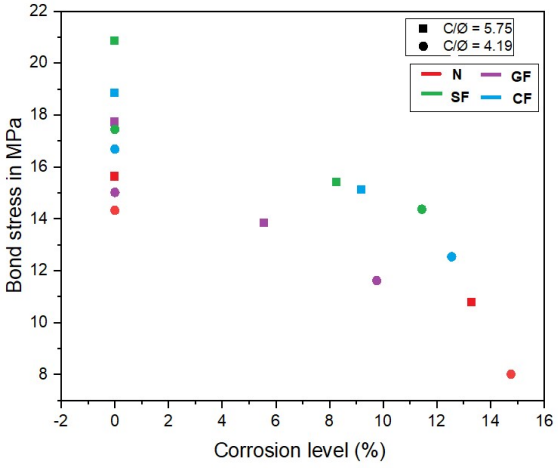

Fig. 9 – Bond stress with different corrosion ratios

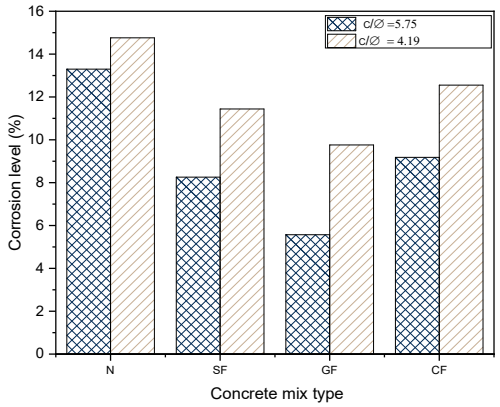

Fig. 10 – Levels of corrosion in various concrete mixtures

to the series C/Ø= 4.19. In particular, for rebars with a corrosion rate of more than 9 percent, the residual bond strength of corroded rebars was not significantly lower than the uncorroded bond strength. Reduced stress on the matrix around the ribs can lead to less matrix deterioration and hence improved confinement, which is the primary benefit[18].

3.4. bond strength

Pull-out testing in accordance with IS 2770 (Part 1) was performed with the bond strength estimated from the load at a measured slip of 0.025 mm and 0.25 mm for deformed bars, respectively. Fig.9 demonstrates the slip's connection strength throughout the course of the whole series. For each series, the bond strength of conventional concrete specimens was found to be lower than the bond strength of fiber-reinforced concrete specimens. The fibers provide the implanted steel rebar with strong confinement. There was a significant difference in bond strength between uncorroded concrete samples and corroded concrete samples when it came to C/Ø = 4.19 series, with the bond strength of uncorroded concrete samples being much higher. When compared to conventional concrete specimens, the bond strength of SF, GF, and CF included specimens rose by 25.07 %, 6.35%, and 13.13% for the C/Ø = 5.75 series. It was demonstrated that the performance of concrete mixes with SF was superior to that of other concrete mixes shown in Fig.9. The C/Ø ratio and the fiber characteristics influence the bond strength of uncorroded concrete specimens[19]. Due to the lower bond strength of the C/Ø = 4.19 series specimens compared to the C/Ø = 5.75 series specimens, the C/Ø ratio matched the bond strength indicated in Fig.9. It was found that the bond strength of the corroded concrete sample was greatly decreased. Corrosion, on the other hand, has grown as illustrated in Fig.9. The bond strength was found to be directly proportional to both the corrosion level and the (C/Ø) ratio. This series had a bond strength ranging from 20.85 to 10.79 MPa, whereas the C/Ø = 4.19 series had one ranging from 17.45 to 9.06 MPa. Due to corrosion, the mechanical interlocking action is reduced, which reduces the bond strength of the damaged ribs In.

Table 3

Pull-out test results

Concrete Mix ID	Ultimate bond stress (τ) in MPa	Corrosion level(υ)in %	Slip(s) in mm
Ø16-N-4.19-Ref	14.33	0	1.55
Ø16-SF-4.19-Ref	17.45	0	1.72
Ø16-GF-4.19-Ref	14.99	0	1.42
Ø16-CF-4.19-Ref	16.67	0	1.98
Ø12-N-5.75-Ref	16.67	0	0.92
Ø12-SF-5.75-Ref	20.85	0	1.56
Ø12-GF-5.75-Ref	17.73	0	1.48
Ø12-CF-5.75-Ref	18.86	0	1.43
Ø16-N-4.19-Cor	9.06	14.76	0.85
Ø16-SF-4.19-Cor	13.37	11.44	1.02
Ø16-GF-4.19-Cor	11.62	9.76	0.92
Ø16-CF-4.19-Cor	12.54	12.55	0.78
Ø12-N-5.75-Cor	10.79	13.3	0.62
Ø12-SF-5.75-Cor	15.42	8.26	1.22
Ø12-GF-5.75-Cor	13.83	5.57	1.13
Ø12-CF-5.75-Cor	15.12	9.18	1.33

addition, compared to the C/Ø = 4.19 series, the C/Ø = 5.75 series had a rather substantial drop in bond strength. C/Ø of 5.75 series bond strength loss is 26.04% for SF, 21.99% and 18.23% integrated concrete specimens when the corrosion ratio is about 9 %. Concrete specimens incorporating GF, SF, and CF show reductions in bond strength of 22.48 %, 23.38 %, and 24.77 % at a corrosion ratio of around 11 % for the C/Ø = 4.19 series. Damage to the ribs has a substantial impact on the bond strength since pull-out operations can interlock the ribs entirely for C/Ø = 5.75. As demonstrated in Table 3, the C/Ø = 4.19 series had reduced mechanical interlocking action but failed to fracture the surrounding fiber-reinforced concrete

The comparison to the results of Lijun Hou et al.[20] on uncorroded confined specimens may indicate how corroded specimens might boost the confinement effect and hence bond strength, but an uncorroded specimen can only ensure a pull-out failure mode.

As per equation(2), all reference samples (uncorroded) with both diameters achieve sufficient bond strength, but corroded conventional concrete samples not achieving sufficient bond strength at the same time all fibers incorporated in corroded samples express sufficient bond strength shown in Table 3.

3.5. Corrosion level (%)

The amount of corrosion in the embedded steel rebar has been determined by the use of weight loss analysis. Initially, the corrosion degree of embedded steel rebar was determined in accordance with Faraday's law, which was implemented using Eq (3). Because the current measurements rose abruptly when the specimens were broken at their bottom surface, the accelerated corrosion tests had to be stopped after 600 hours of running time. The corroded steel rebar was ejected from the concrete specimen at the conclusion of the pull-out experiment in order to determine the weight loss of the specimens. The rusted rebars have been thoroughly cleaned in accordance with ASTM G01-03. The degree of corrosion in steel rebar was measured by using Eq (3). In the SF concrete mix specimens, corrosion had a substantial impact on the steel bars contained in the concrete mix. The corrosion effects of reinforced concrete specimens immersed in E-glass fiber inclusion concrete mix, on the other hand, were significantly reduced. Perhaps because SF and CF are metallic fibers and strong electric conductors, the electrical charge travelling through SF and CF-integrated concrete specimens are greater than that passing through GF-incorporated concrete specimens[21], although the explanation for this is not entirely clear. Each of the specimens had a different amount of corrosion, which is illustrated in Table 3. Fig.1 shows that the corrosion level of fibers inserted in concrete mix specimens was lower than the corrosion level of conventional concrete specimens in each of the series (C/5.25 and C/4.19, respectively) shown in Fig.10. The glass fibers corrosion level results were in line with previous experimental results reported in Ramanathan et al. [22].

In this experiment, its observed steel fibers where contact with the embedded rebar those fibers were only corroded, and the remaining fibers were not corroded.

4.Conclusions

The following conclusion was drawn from the study:

1. The use of fibers in concrete at a rate of 1% of the total volume results in excellent confinement, which decreases corrosion-induced cracking. The confinement effect was more clearly observed in specimens with a lower C/Ø ratio than in others.
2. Accelerated corrosion resulted in typical concrete specimens with fracture widths and depths of 0.15 to 0.25 millimetres (mm). When it came to resistance to chloride attack, fiber reinforced concrete specimens outperformed

conventional specimens, especially those prepared with GF inclusion concrete mix, which performed better than specimens prepared with SF or CF.

3. Increased bonding between steel rebar and the concrete matrix is observed when fibers such as SF, GF, and CF are added to concrete mix specimens, particularly when SF concrete mix specimens with C/Ø = 5.75 are used. In the case of uncorroded rebar, increasing the C/Ø increased the bonding strength between steel rebar and concrete specimens.
4. The bond strength decreased in a linear fashion as the corrosion ratio rose. The loss of bond strength caused by rebar corrosion was shown to be related to the ratio C/Ø as well as the mechanism of failure. Because of the significant bond strength loss (about 27% at a corrosion rate of 13.39 %), specimens with C/Ø = 5.75 failed by pull-out and demonstrated a high bond strength loss of roughly 27%. While C/Ø = 4.19, the failure mechanism of the specimens was the combined split and pull-out, which resulted in a loss of 24.77% at a corrosion rate of 12.9%, according to the results.
5. Corrosion-induced residual bond strength was found to be greater than that of uncorroded rebars, particularly for rebars with corrosion rates of more than 9.0%, according to the findings. It can result in reduced amounts of stress on the matrix around the ribs, resulting in less matrix degradation and, ultimately, better confinement.

REFERENCES

[1] X. H. Wang, X. H. Gao, B. Li, and B. R. Deng, "Effect of bond and corrosion within partial length on shear behaviour and load capacity of RC beam," *Constr. Build. Mate,*2011, **25**(4), 1812–1823.

[2] S. Yin, L. Jing, and H. Lv, "Experimental Analysis of Bond between Corroded Steel Bar and Concrete Confined with Textile-Reinforced Concrete," *J. Mater. Civ. Eng*, 2019, **31(**10).

[3] G. N. Gopu and A. Sofi, "Electrical Waste Fibers Impact on Mechanical and Durability Properties of Concrete," *Civ. Eng. Archit*, 2021, **9**(6), 1854–1868.

[4] P. Kittl, E. Galleguillos, and G. Diaz, "Properties of compacted copper fibre reinforced cement composite," *Int. J. Cem. Compos. Light. Concr*, 1985, **7**(3), 193–197.

[5] S. Patel, R. S. Rana, and S. K. Singh, "Study on mechanical properties of environment friendly Aluminium E-waste Composite with Fly ash and E-glass fiber," *Mater. Today Proc*, 2017, **4**(2),3441–3450.

[6] D. Das, O. P. Dubey, M. Sharma, R. K. Nayak, and C. Samal, "Mechanical properties and abrasion behaviour of glass fiber reinforced polymer composites – A case study," *Mater. Today Proc*, 2019, **19**, 506–511.

[7] A. Sofi and G. Naidu Gopu, "Influence of steel fibre, electrical waste copper wire fibre and electrical waste glass fibre on mechanical properties of concrete," *IOP Conf. Ser. Mater. Sci. Eng.*,2019, **513** (1).

.[8] V. Marcos-Meson, A. Solgaard, G. Fischer, C. Edvardsen, and A. Michel, "Pull-out behaviour of hooked-end steel fibres in cracked concrete exposed to wet-dry cycles of chlorides and carbon dioxide – Mechanical performance," *Constr. Build. Mater.*,2020, **240**, 117764.

[9] BIS:10262, "Indian Standard Guidelines for concrete mix design proportioning," *Bur. Indian Stand. New Delhi*, p. New Delhi,India, 2009.

[10] F. Tondolo, "Bond behaviour with reinforcement corrosion," *Constr. Build. Mater.*,2015, **93**, 926–932.

[11] N. A. Farhan, M. N. Sheikh, and M. N. S. Hadi, "Experimental Investigation on the Effect of Corrosion on the Bond Between Reinforcing Steel Bars and Fibre Reinforced Geopolymer Concrete," *Structures*, **14**, 251–261.

[12] RILEM TC, "AAC 8.2 Push-out test for reinforcement," in *RILEM Recommendations for the Testing and Use of Constructions Materials*, RILEM, Ed. E & FN SPON, 1992, 141–142.

[13] C. Andrade, M. Prieto, P. Tanner, F. Tavares, and R. D'Andrea, "Testing and modelling chloride penetration into concrete," in *Construction and Building Materials*, 2013, **39**, pp. 9–18.

[14] G. N. Gopu and S. A. Joseph, "Corrosion Behavior of Fiber-Reinforced Concrete—A Review," *Fibers 2022, **10**, 38.*

[15] C. G. Berrocal, I. Löfgren, and K. Lundgren, "The effect of fibres on steel bar corrosion and flexural behaviour of corroded RC beams," *Eng. Struct.*, 2018, **163**, 409–425.

[16] L. Hou, Y. Li, J. Sun, S. H. Zhang, H. Wei, and Y. Wei, "Enhancement corrosion resistance of MgAl layered double hydroxides films by anion-exchange mechanism on magnesium alloys," *Appl. Surf. Sci.*,2019, **487**, 101–108.

[17] H. Fazli, A. Y. M. Yassin, N. Shafiq, and W. Teo, "Pull-off testing as an interfacial bond strength assessment of CFRP-concrete interface exposed to a marine environment," *Int. J. Adhes. Adhes.*,2018, **84**, 335–342.

[18] G. N. Gopu and A. Sofi, "The influence of fiber RC beams under flexure on the chloride-induced corrosion," *Case Stud. Constr. Mater.*,2022, **17**, e01566.

[19] H. Lin *et al.*, "State-of-the-art review on the bond properties of corroded reinforcing steel bar," *Construction and Building Materials*,2019, **213**, 216–233.

[20] L. Hou, B. Zhou, S. Guo, N. Zhuang, and D. Chen, "Bond-slip behavior between pre-corroded rebar and steel fiber reinforced concrete," *Constr. Build. Mater.*,2018, **182**, 637–645.

[21] D. Y. Yoo, J. Y. Gim, and B. Chun, "Effects of rust layer and corrosion degree on the pullout behavior of steel fibers from ultra-high-performance concrete," *J. Mater. Res. Technol*, 2020, **9** (3), 3632–3648.

[22] S. Ramanathan, V. Benzecry, P. Suraneni, and A. Nanni, "Condition assessment of concrete and glass fiber reinforced polymer (GFRP) rebar after 18 years of service life," *Case Stud. Constr. Mater.*,2021,**14.**

****